

Predicting scaling properties of fluids from individual configurations: Small molecules

Zahraa Sheydaafar,^{*} Jeppe C. Dyre, and Thomas B. Schrøder[†]

*Glass and Time, IMFUFA, Department of Science and Environment,
Roskilde University, P.O. Box 260, DK-4000 Roskilde, Denmark*

(Dated: February 10, 2024)

Abstract

Isomorphs are curves in the phase diagram along which both structure and dynamics to a good approximation are invariant. There are two main methods to trace out isomorphs in both atomic and molecular systems, the configurational adiabat method and the direct isomorph check method. We introduce and test a new family of force based methods on three molecular models; the asymmetric dumbbell model, the symmetric inverse power law dumbbell model, and the Lewis-Wahnström model of o-terphenyl. A unique feature of the force based methods is that they only require a single configuration to trace out an isomorph. The atomic force method was previously shown to work very well for the Kob-Andersen binary Lennard-Jones mixture, but we show that it does not work for molecular models. In contrast, we find that a new method based on molecular forces works well for all three molecular models.

PACS numbers: Valid PACS appear here

^{*} samaneh@ruc.dk

[†] tbs@ruc.dk

I. INTRODUCTION

Isomorphs are curves of invariant structure and dynamics in the thermodynamic phase diagram. They occur in systems with strong correlations between the constant-volume canonical-ensemble equilibrium fluctuations of potential energy and virial [1, 2], which characterize the so-called R-simple (strongly correlating) systems [3–6]. The Pearson correlation coefficient R between the thermal equilibrium fluctuations of potential energy U and virial W is given by (where sharp brackets denote NVT canonical averages, and ‘ Δ ’ denotes the deviation from equilibrium mean value, e.g., $\Delta U \equiv U - \langle U \rangle$):

$$R = \frac{\langle \Delta W \Delta U \rangle}{\sqrt{\langle (\Delta W)^2 \rangle \langle (\Delta U)^2 \rangle}}. \quad (1)$$

For an inverse power-law (IPL) system with pair potential proportional to r^{-n} in which r is the pair distance, the correlation is perfect, $R = 1$, because $W = (n/3)U$ for all microconfigurations. Somewhat smaller correlations still lead to fairly invariant structure and dynamics, and the class of R-simple liquids is defined by $R > 0.9$. Isomorph theory has been applied to different classes of systems, including simple atomic systems in both liquid and solid phases [7, 12–17], molecular systems [18], and the 10-bead Lennard-Jones chain [19]. Furthermore, isomorph-theory predictions have been verified in experiments on van der Waals bonded organic liquids [20, 21].

In 2012, Ingebrigtsen and et al. [18] studied isomorphs for liquid molecular systems composed of small rigid molecules. They found isomorphs in the asymmetric dumbbell model (ASD) (Fig. 1(a)), the symmetric inverse power law (IPL) dumbbell model (Fig. 1(b)), and the Lewis- Wahnström o-terphenyl (OTP) model (Fig. 1(c)). It is important to note that isomorph invariances refer to structure and dynamics reported in the so-called *reduced* (state-point dependent) units. In this unit system, the length unit l_0 is defined by the particle number density $\rho \equiv N/V$ where N is the particle number and V the system volume, the temperature T defines the energy unit e_0 , and the density and the thermal velocity define the time unit t_0 . Thus if m is the particle mass, the length, energy, and time units are given [1, 3, 7] by

$$l_0 = \rho^{-1/3}, \quad e_0 = k_B T, \quad t_0 = \rho^{-1/3} \sqrt{m/k_B T}. \quad (2)$$

Reference 18 used the so-called configurational adiabat method to trace out isomorphs. For

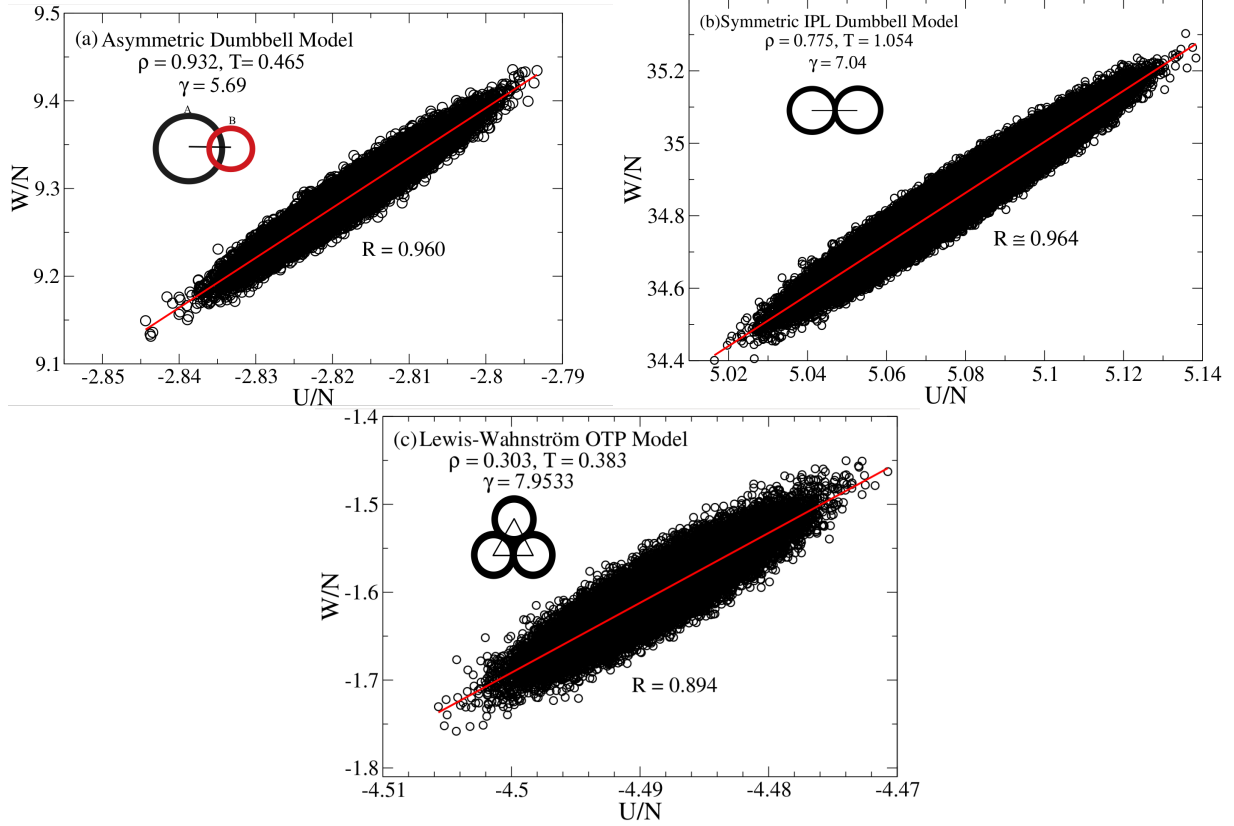


FIG. 1. The fluctuation of potential energy and virial for the asymmetric dumbbell and symmetric IPL dumbbell models and the OTP model with rigid bonds. (a) The Pearson correlation coefficient at the reference state point $(\rho_1, T_1) = (0.932, 0.465)$ is $R = 0.959$ and the linear slope of regression is $\gamma = 5.69$ for the asymmetric dumbbell model. (b) $R = 0.962, \gamma = 7.11$ for the symmetric dumbbell model at state point $(\rho_1, T_1) = (0.806, 1.400)$. (c) $R = 0.894, \gamma = 7.95$ for the OTP model at state point $(\rho_1, T_1) = (0.303, 0.383)$.

a scatter plot of virial versus potential energy of configurations taken from an equilibrium simulation (see Fig. 1), the linear-regression slope γ is given [7–10] by

$$\gamma \equiv \frac{\langle \Delta U \Delta W \rangle}{\langle (\Delta U)^2 \rangle} = \left(\frac{\partial \ln T}{\partial \ln \rho} \right)_{S_{\text{ex}}} . \quad (3)$$

Recall that S_{ex} is the total entropy minus ideal gas entropy at the same density and temperature ($S_{\text{ex}} < 0$ due to the fact that any system is more ordered than an ideal gas). For R-simple liquids, the isomorph theory predicts invariance of the dynamics along the configurational adiabats defined by $S_{\text{ex}} = \text{Const}$ [18, 28–30]. For any system, Eq. (3) allows one to generate the configurational adiabats. This is done by calculating the two canonical averages

in Eq. (3) at an initial state point, changing density slightly, and from Eq. (3) calculating the corresponding change in temperature. At the new state point the canonical averages are recalculated, and so on.

Another method to generate isomorphs is termed the direct isomorph check, which works as follows. Two configurations of the strongly correlated system have proportional Boltzmann factors, i.e.

$$e^{-U(\mathbf{R}^{(1)})/k_B T_1} = C_{12} e^{-U(\mathbf{R}^{(2)})/k_B T_2}. \quad (4)$$

Here $\mathbf{R}^{(1)}$ and $\mathbf{R}^{(2)}$ are two configurations that scale uniformly into one another, $\mathbf{R}^{(2)} = (\rho_1/\rho_2)^{1/3} \mathbf{R}^{(1)}$, and C_{12} is a constant that depends only on the two state points in question. By taking the logarithm of Eq. (4) we get

$$U(\mathbf{R}^{(2)}) = \frac{T_2}{T_1} U(\mathbf{R}^{(1)}) + k_B T_2 \ln C_{12}. \quad (5)$$

Thus, taking configurations, $\mathbf{R}^{(1)}$, from an equilibrium NVT simulations at (ρ_1, T_1) and plotting $U(\mathbf{R}^{(2)})$ versus $U(\mathbf{R}^{(1)})$ is predicted to reveal strong correlation, and T_2 can be calculated from the slope.

Below, we investigate new efficient methods for generating isomorphs. They are all based on the scaling properties of a single configuration selected from an equilibrium simulation of a reference state point. This works well for the Kob-Andersen binary Lennard-Jones mixture, which is a R-simple system [23]. The present paper extends the single-configuration idea to deal with three molecular system: the asymmetric dumbbell (ASD) model, the symmetric inverse power law (IPL) dumbbell model, and the Lewis-Wahnström OTP model.

II. SIMULATION DETAILS

We studied three molecular systems with rigid bonds, the asymmetric dumbbell model ($N = 5000$), symmetric IPL dumbbell r^{-18} model ($N = 5000$), and the Lewis-Wahnström OTP model ($N = 3000$). All three models were previously shown to have good isomorphs [18].

Asymmetric dumbbell molecules consist of two different sized Lennard-Jones (LJ) spheres, a large (A) and a small (B) particle, rigidly bonded. The length of the bonds is 0.584 in the LJ units defined by the large sphere ($\sigma_{AA} \equiv 1$, $\epsilon_{AA} \equiv 1$, and $m_A \equiv 1$). The parameters

of the model were chosen to mimic toluene ($\sigma_{AB} = 0.894$, $\sigma_{BB} = 0.788$, $\epsilon_{AB} = 0.342$, $\epsilon_{BB} = 0.117$, $m_B = 0.195$) [28]. The inter-molecular pair potential interactions are given by the Lennard-Jones pair potential:

$$v_{ij}(r_{ij}) = 4\epsilon_{ij} \left[\left(\frac{\sigma_{ij}}{r_{ij}} \right)^{12} - \left(\frac{\sigma_{ij}}{r_{ij}} \right)^6 \right]. \quad (6)$$

The symmetric IPL model consists of two identical particles, connected by a rigid bond of length 0.584. The inter-molecular pair potential interactions are given by the inverse power-law (IPL) potential:

$$v_{ij} = \epsilon_{ij} \left(\frac{\sigma_{ij}}{r_{ij}} \right)^n \quad (7)$$

in which $n = 18$. All IPL parameters and particle masses are unity.

The Lewis-Wahnström OTP model consists of three identical LJ particles. Atoms are connected by rigid bonds in an isosceles triangle with side length 1.000 and a top angle of 75° . All LJ parameters are set to unity in this model either.

All Molecular Dynamics simulations were performed in the NVT ensemble with a Nose-Hoover thermostat using RUMD, an open-source package that can be downloaded at <http://rumd.org> [24].

III. THREE SINGLE-CONFIGURATION METHODS FOR IDENTIFYING ISOMORPHS

Generating isomorphs by means of Eq. (3) for an R-simple system is straightforward but requires, as the numerical calculation of most statistical-mechanical quantities, a time sequence of equilibrium configurations. Good statistics can be obtained, however, from the scaling properties of the forces of a single configuration [23]. The idea is to make use of the fact that *all* reduced forces are isomorph invariant.

To show that the reduced forces are all invariant along an isomorph, we refer to the basic equation of isomorph theory [11],

$$U(\mathbf{R}) = U(\rho, S_{\text{ex}}(\tilde{\mathbf{R}})). \quad (8)$$

Here $\mathbf{R} \equiv (\mathbf{r}_1, \dots, \mathbf{r}_N)$ is the configuration vector of all particle coordinates, $U(\rho, S_{\text{ex}})$ is the thermodynamic average potential energy at the state point with density ρ and excess entropy

S_{ex} , $\tilde{\mathbf{R}} \equiv \rho^{1/3}\mathbf{R}$ is the reduced configuration vector, and $S_{\text{ex}}(\tilde{\mathbf{R}})$ is the microscopic excess-entropy function as defined in Ref. 11. The fact that the latter function depends only on the configuration's *reduced* coordinates is a consequence of the hidden scale invariance condition $U(\mathbf{R}_a) < U(\mathbf{R}_b) \Rightarrow U(\lambda\mathbf{R}_a) < U(\lambda\mathbf{R}_b)$ in which λ is a uniform scaling parameter [11]. This condition is equivalent to the system having strong virial potential-energy correlations [7].

It follows from Eq. (8) that the vector of all forces on the individual particles, $\mathbf{F} \equiv (\mathbf{F}_1, \dots, \mathbf{F}_N)$, is given by

$$\mathbf{F}(\mathbf{R}) = -\nabla U(\mathbf{R}) = -\left(\frac{\partial U}{\partial S_{\text{ex}}}\right)_\rho \rho^{1/3} \tilde{\nabla} S_{\text{ex}}(\tilde{\mathbf{R}}). \quad (9)$$

Since $(\partial U / \partial S_{\text{ex}})_\rho = T$, the reduced force vector $\tilde{\mathbf{F}} \equiv l_0 \mathbf{F} / e_0 = \rho^{-1/3} \mathbf{F} / k_B T$ is given by (where $\tilde{S}_{\text{ex}} \equiv S_{\text{ex}} / k_B$)

$$\tilde{\mathbf{F}} = -\tilde{\nabla} \tilde{S}_{\text{ex}}(\tilde{\mathbf{R}}). \quad (10)$$

The fact that $\tilde{\mathbf{F}}$ depends only on the *reduced* coordinates implies invariant dynamics along an isomorph because in this case, the reduced-unit version of Newton's second law, $d^2 \tilde{\mathbf{R}} / d\tilde{t}^2 = \tilde{\mathbf{F}}(\tilde{\mathbf{R}})$ [1], has no reference to the state point density. This implies invariant reduced dynamics along the isomorphs.

Given a reference state point (ρ_1, T_1) and a new density, ρ_2 , we now derive the equation for calculating the temperature T_2 so that the state point (ρ_2, T_2) is isomorphic with (ρ_1, T_1) . If \mathbf{R}_1 is a configuration taken from an equilibrium simulation of the reference state point and \mathbf{R}_2 is the same configuration scaled uniformly to density ρ_2 , the fact that the reduced forces of the two configurations are identical is expressed as follows:

$$\tilde{\mathbf{F}}(\mathbf{R}_1) = \tilde{\mathbf{F}}(\mathbf{R}_2). \quad (11)$$

From this identity T_2 can be determined by:

$$T_2 = \frac{|\mathbf{F}(\mathbf{R}_2)|}{|\mathbf{F}(\mathbf{R}_1)|} \left(\frac{\rho_1}{\rho_2}\right)^{1/3} T_1. \quad (12)$$

The atomic force method was tested for the Kob-Andersen binary Lennard-Jones model in Ref [23]. For a system composed of rigid bonded molecules, in addition to atoms' forces, the center-of-mass forces are expected to be isomorph invariant in reduced units. This paper tests both force methods on the ASD, IPL and OTP systems. The method is illustrated

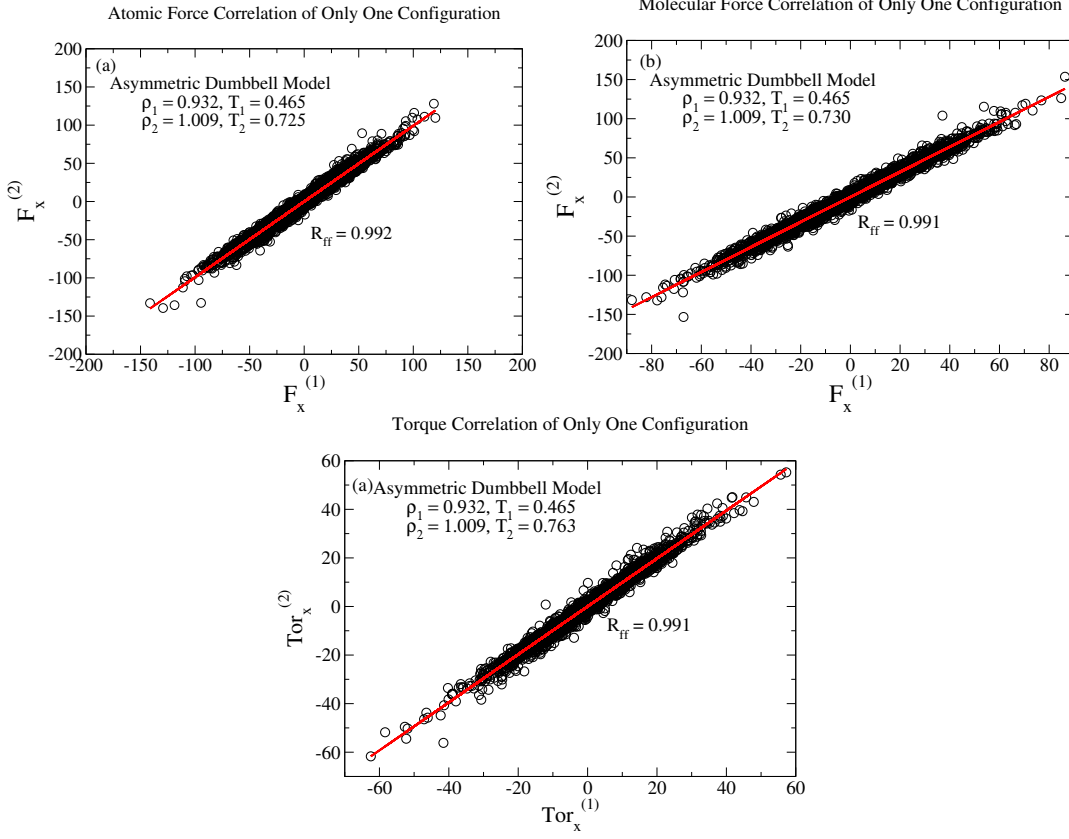


FIG. 2. (a) [“atomic-force method”] shows a plot of all particle forces in one axis direction for a single configuration \mathbf{R}_1 of the reference state point $(\rho_1, T_1) = (0.932, 0.465)$ versus for its uniformly scaled version to density ρ_2 , $\mathbf{R}_2 = (\rho_1/\rho_2)^{1/3}\mathbf{R}_1$. From the slope of the best-fit line via Eq. (12) one identifies $T_2 = 0.725$. (b) [“molecular-force method”] shows a similar plot based on the center-of-mass forces between the molecules (which ignores the intramolecular forces). Better correlation is obtained here, and the slightly different $T_2 = 0.730$ is arrived at using this method. (c) [“Torque Method”] shows the same plot in regard to the rotational motion of molecules. Despite the approximately same correlation, the temperature defined from this method Eq. (13) is quite different, $T_2 = 0.763$.

in Fig. 2 in which (a) for the ADP system shows the x-coordinates of the forces on all particles plotted against the same quantities of the uniformly scaled configuration for a 7% density increase. (b) shows the same for the center-of-mass “molecular” forces between the molecules, which have no contributions from the intramolecular forces. We find a strong correlation in both cases, but a somewhat different prediction for T_2 , which is 0.725 by using atomic force method and 0.730 by using center-of-mass force method.

Before comparing the two methods by testing for invariant dynamics, we introduce a third method based on the isomorph invariance of the reduced-unit torque on each molecule, i.e., $\tilde{\tau}_1 = \tilde{\tau}_2$ where τ is the torque. Since the torque in reduced units is defined by $\tilde{\tau} \equiv \tau/e_0 = \tau/k_B T$, the invariance requirement means that T_2 is given by

$$T_2 = \frac{|\tau_2|}{|\tau_1|} T_1. \quad (13)$$

This assumes invariance of the reduced rotational dynamics of the particles around the molecules' center-of-mass. This method is used in Fig. 2(c), which shows a quite high correlation of the torques before and after scaling the configuration, but a somewhat higher temperature, $T_2 = 0.763$.

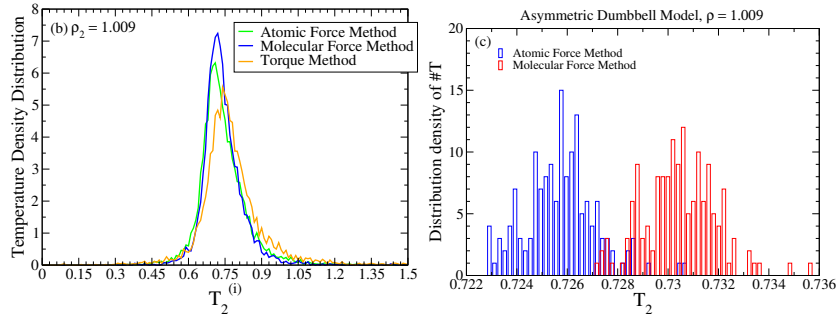


FIG. 3. (a) Distribution of temperatures predicted by applying Eq. (12) and Eq. (13) to individual molecules in a single configuration. For perfect scaling, all the molecules should 'agree', i.e., the distributions should be delta functions. (b) the distribution of T_2 values predicted from 152 independent configurations by using the atomic force (blue) and molecular force (red) methods.

Fig. 3(a) shows the distribution of T_2 predictions, when Eq. (12) and Eq. (13) are applied to individual molecules. The width of the distributions are similar, but smallest for the molecular-force method. Fig. 3(b) shows the distribution of T_2 values predicted by applying Eq. (12) to 152 independent configurations. Using one configuration is a main advantage of the new force based methods considered here. However, for comparison between the methods, we will in the following use the average of the T_2 values predicted from 100-200 independent configurations.

IV. RESULTS

In the following we will test the three different methods on the three models introduced above. Both translational and rotational dynamics is considered; we test the invariance of the reduced molecular center-of-mass mean square displacement (msd), the intermediate incoherent scattering function (Fs), and the orientational time-autocorrelation function.

Tests of the three methods on ASD are shown in Fig. 4. The state point $(\rho_1, T_1) = (0.932, 0.465)$ is the reference point. From this we determined two state points with lower density and two with higher density, spanning in all a density variation of 19%. The configuration was scaled uniformly to the relevant density ρ_2 in order to determine the temperature T_2 at which the reduced forces/torques are the same as at the reference state point. The best results are obtained with the molecular-force method (Fig. 4 (d), (e), and (f)).

TABLE I. Reduced-unit density variation of the diffusion coefficient (first row), the relaxation time of molecular center-of-mass dynamics (second row) and rotational dynamics (third row) for the ASD model. The second column shows large numbers arising from the isotherm, non-invariant curves. The third to seventh columns represent the configurational adiabat, direct isomorph check, atomic and molecular forces and torque methods. The molecular force method is better than other methods for predicting state points of approximately invariant dynamics.

	Isotherm	γ	DIC	F_{Atom}	F_{Mol}	Torque
$\frac{\partial \log \tilde{D}}{\partial \log \rho}$	-70(2)	-0.5(4)	1.1(4)	-1.4(2)	-0.9(4)	7.47(6)
$\frac{\partial \log \tilde{\tau}_{cm}}{\partial \log \rho}$	77(3)	-0.4(1)	-1.0(1)	1.60(7)	0.5(1)	-7.8(1)
$\frac{\partial \log \tilde{\tau}_{rot}}{\partial \log \rho}$	65(3)	1.9(1)	1.26(2)	3.47(3)	2.62(7)	-2.6(2)

Figure 5 shows the variation of the relaxation times of translational motion (a) and rotational motion (b) for an isotherm (purple), configurational adiabat (black), as well as curves generated by the direct isomorph check (red), atomic force (green), molecular force (blue), and torque methods (orange). Not surprisingly, all the approximate isomorphs are better in representing the invariant relaxation compared to the isotherm. Table I shows the density variation of the diffusion coefficient and translational and rotational relaxation times (first column) in reduced units along the isotherm (second column) and the five approximate isomorphs (third-seventh columns). The diffusion coefficient is calculated from the diffusive

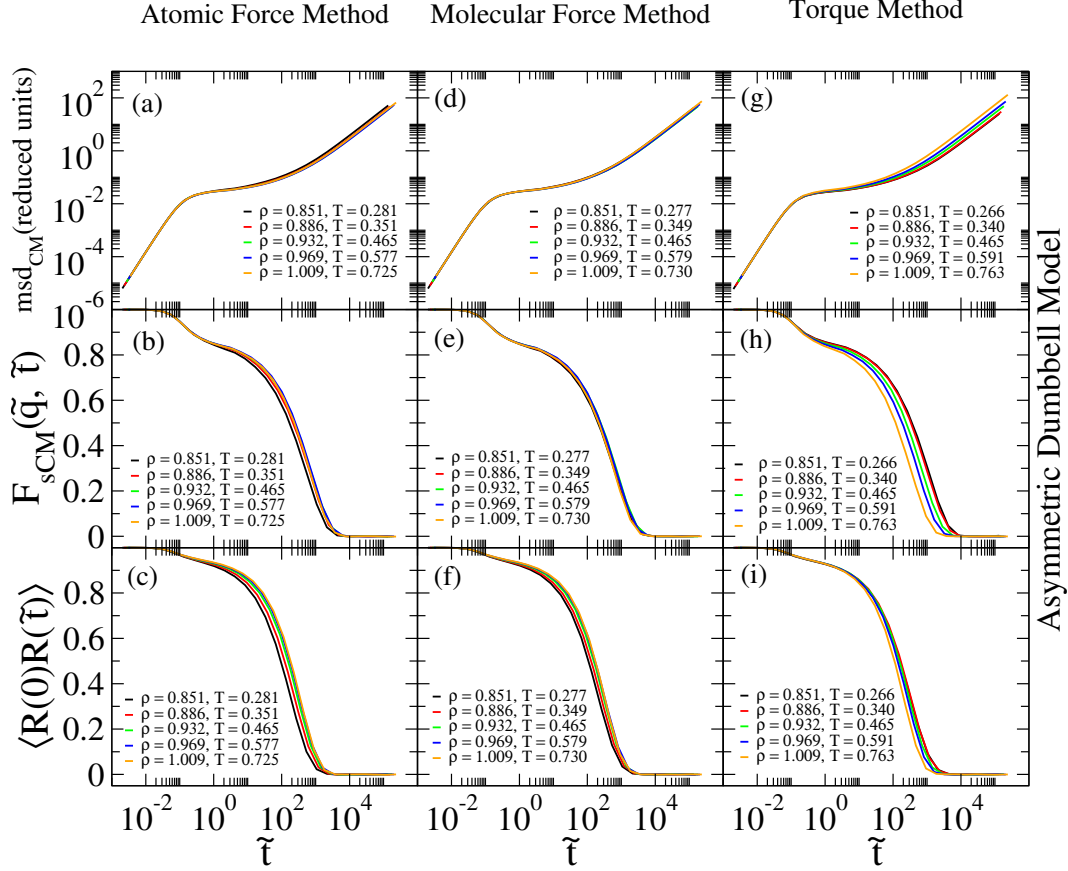


FIG. 4. Testing the ASD model for invariance of the reduced translational and rotational dynamics by three different methods. Each method investigates the reduced center-of-mass mean-square displacement (upper figures), the center-of-mass incoherent intermediate scattering function for the reduced wave-vector $\tilde{q} = q(\rho/0.932)^{1/3}$ (middle figures), and the orientational time-autocorrelation function probed via the autocorrelation of the normalized bond vector (bottom figures). (a), (b), (c) show results for state points generated by the atomic-force method based on requiring invariant reduced forces between all atoms, including the intramolecular contributions (Eq. (12)). (d), (e), (f) show results for state points generated by the molecular-force method requiring invariant reduced center-of-mass forces between the molecules (Eq. (12)). (g), (h), (i) show results for state points generated by the torque method requiring invariant reduced torques on the molecules (Eq. (13)).

part of the mean-square displacement (compare Fig. 4). The variation of relaxation times as functions of density are obtained by calculating the slope of relaxation curves of Fig. 5(a) and (b) at two-state points, lower $\rho = 0.886$ and upper $\rho = 0.969$ points of reference state point.

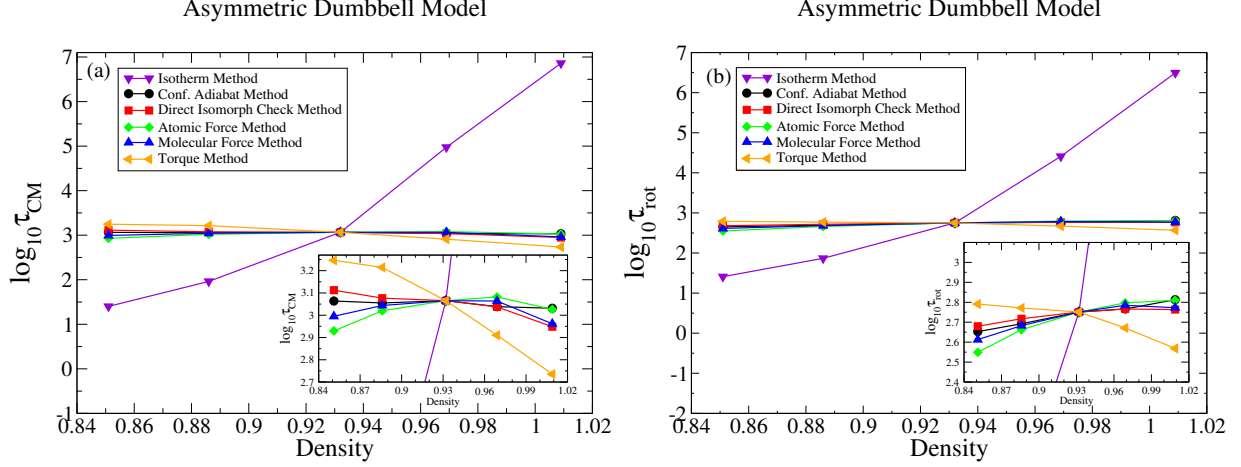


FIG. 5. Comparing the relaxation time as a function of the density for the ASD model along an isotherm (purple) as well as for five different methods: configurational adiabatic (black), direct isomorph check (red), atomic (green) and molecular (blue) force and torque (orange) methods. (a) shows the translational relaxation time calculated by the intermediate scattering function. (b) shows a similar plot for the rotational relaxation time (derived from the orientational time-autocorrelation function of the molecular end-to-end vector).

TABLE II. Checking the reduced-units variation of the same dynamic quantities as in Table I for the symmetric dumbbell IPL model.

	Isotherm	γ	DIC	F_{Atom}	F_{Mol}	Torque
$\frac{\partial \log \tilde{D}}{\partial \log \rho}$	-113.4(6)	1.9(1)	-0.78(7)	-0.2(2)	-0.462(5)	3.9(3)
$\frac{\partial \log \tau_{cm}}{\partial \log \rho}$	126.7(7)	-0.4(3)	-0.04(2)	-0.21(7)	-0.42(1)	-0.95(4)
$\frac{\partial \log \tau_{rot}}{\partial \log \rho}$	107.9(6)	0.16(1)	-0.7(2)	0.2(2)	0.10(9)	0.5(3)

An important question is whether the molecular geometry determines which method work for which model or not. The second model we consider is the IPL symmetric dumbbell model to check the invariance properties by use of the single-configuration force methods. The corresponding quantities are shown in Fig. 6, Fig. 7 and Tabel II. We determine two state point with lower density and two with higher density, spanning in all a density variation of 19%. Overall, for the ASD model we find the molecular force approach to produce the best invariance curves. Fig. 7 (a) and (b) represent the variation of both translational and rotational dynamics by plotting both relaxation times.

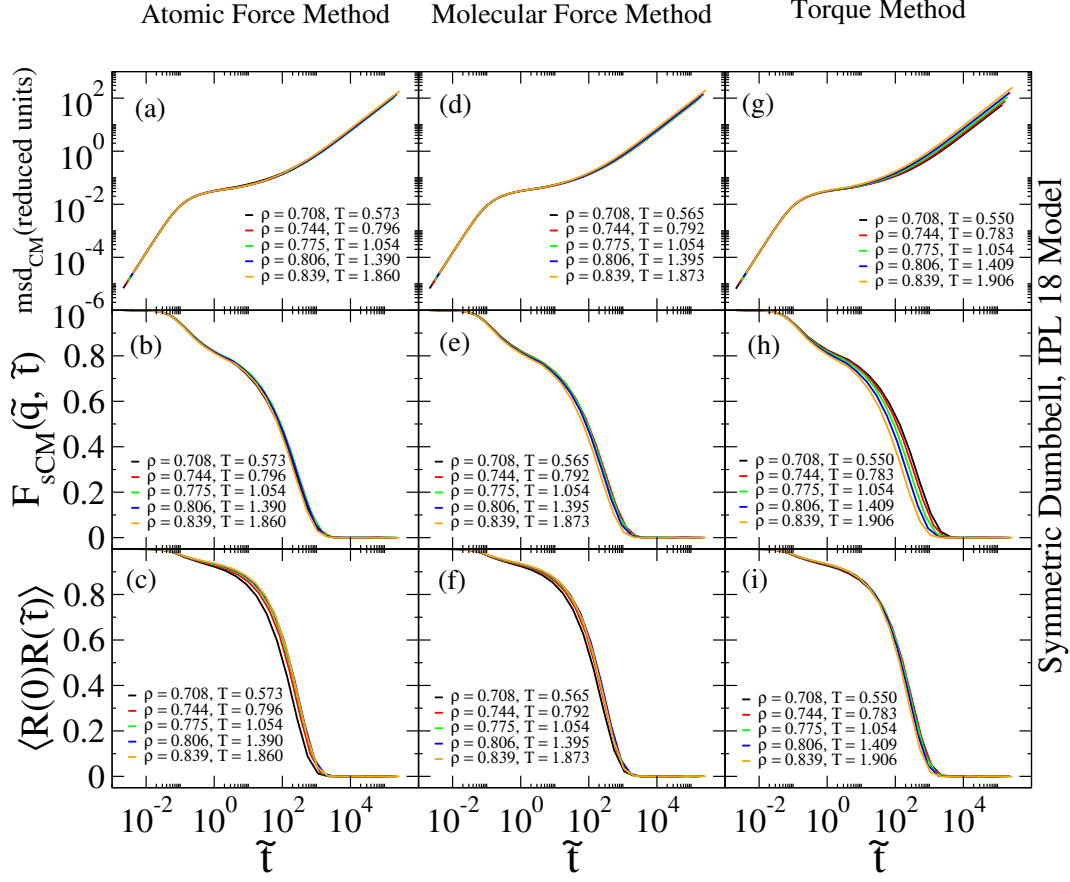


FIG. 6. Testing the atomic force, molecular force, and torque methods on the IPL model for invariance of the reduced translational and rotational dynamics. The same dynamic quantities as in Fig. 4 are investigated. The reference point is $(\rho_1, T_1) = (0.775, 1.054)$ and the values of q considered are constant in reduced units, $\tilde{q} = q(\rho/0.775)^{1/3}$. (a), (b), (c) show results for state points generated by the atomic-force method (which includes the intramolecular contributions, Eq. (12)). (d), (e), (f) show results for state points generated by the molecular-force method (Eq. (12)). (g), (h), (i) show results for state points generated by the torque method (Eq. (13)).

So far, the molecular force method has given the best results. We proceed to investigate the three force methods for the OTP model (Fig. 8). In this model, $(\rho_1, T_1) = (0.303, 0.383)$ is the reference point. The same quantities as before are plotted against the reduced time. Again the molecular force method is best for producing approximate isomorphs (Fig. 9).

There is an interesting distinction in regard to which densities are used to analyze the dynamics. Scaling the OTP system to lower density disturbs the prediction process. In Fig. 10(a) we consider the fourth point of the state points of Fig. 8 (d), $(\rho_1, T_1) =$

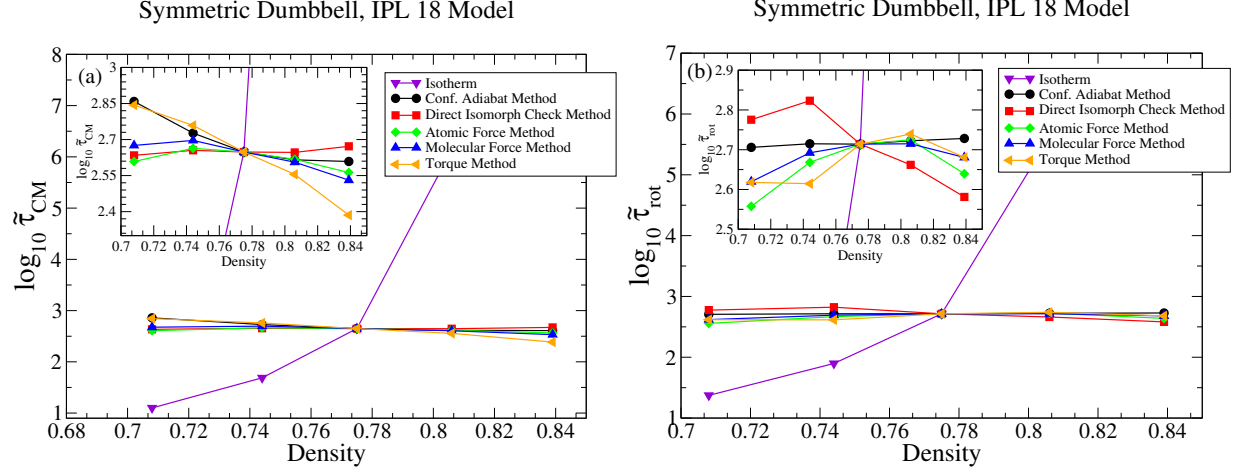


FIG. 7. Comparing the relaxation time as a function of the density for the IPL model along similar curves as in Fig. 5. As shown before, all the approximate isomorph methods are better in representing the invariant relaxation time than the isotherm. (a) shows the translational relaxation time calculated by the intermediate scattering function. (b) shows a similar plot for rotational relaxation time.

(0.340, 0.903), as reference point, and then move to lower densities, spanning about 16%. The invariant intermediate scattering function in Fig. 8 has disappeared by decreasing densities in Fig. 10. On the other hand, the approaches are able to give the proper curves only if scaling the configuration to higher density in OTP system. This issue is only found in OTP model, not the other two models. For example, the IPL model dynamics has been still invariant in reduced units along the molecular force methods. Figure 10(b) shows the reduced incoherent intermediate scattering function of isomorphs points when we start from $(\rho_1, T_1) = (0.806, 1.395)$ (Fig. 6(e)) and decrease the density. The dynamics of IPL model is still invariant however it gives the different state points in comparison with Fig. 6(e) because the isomorphs are approximate.

To investigate the OTP model issue, we calculate the translational and rotational relaxation times through the isotherm and isomorphs methods by decreasing the density (Figure 11). By scaling the configurations to lower density, the configurational adiabats and DIC methods still create the isomorphs along which the dynamics is quite invariant. However, this is clearly not the case for the force methods. Thus, for the OTP model the molecular force method works well, but only if increasing density from the reference point. At the present we do not have an explanation for this

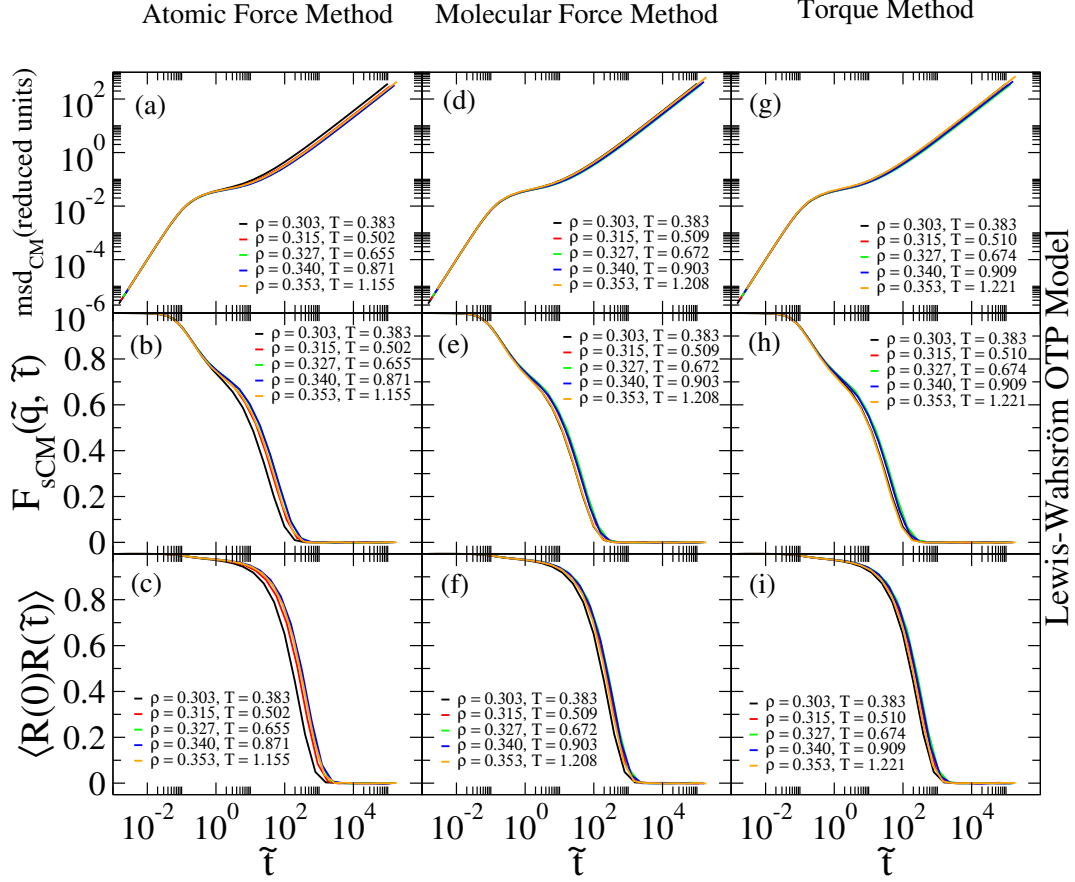


FIG. 8. Testing for invariance of the same reduced dynamics as in Fig. 4 and Fig. 6 for the OTP model. Approximate isomorphs were generated based on a single equilibrium configuration from the reference state point $(\rho_1, T_1) = (0.303, 0.383)$. Results were averaged over 152 configurations to improve statistics. (a), (b), (c) show results for state points generated by the atomic-force method. (d), (e), (f) show results for state points generated by the molecular-force method. (g), (h), (i) show results for state points generated by the torque method.

V. DISCUSSION

Isomorphs exist in systems with strong virial potential-energy correlation, including molecular systems with rigid bonds. For the asymmetric dumbbell, the symmetric dumbbell, and the Lewis-Wahnström OTP models, we have seen that there exists curves along which the dynamics is invariant to a good approximation. Though not our focus here, we note that the structure is invariant to a good approximation for all three methods (Fig. 12).

We tested several methods to generate an approximate isomorph starting from a given

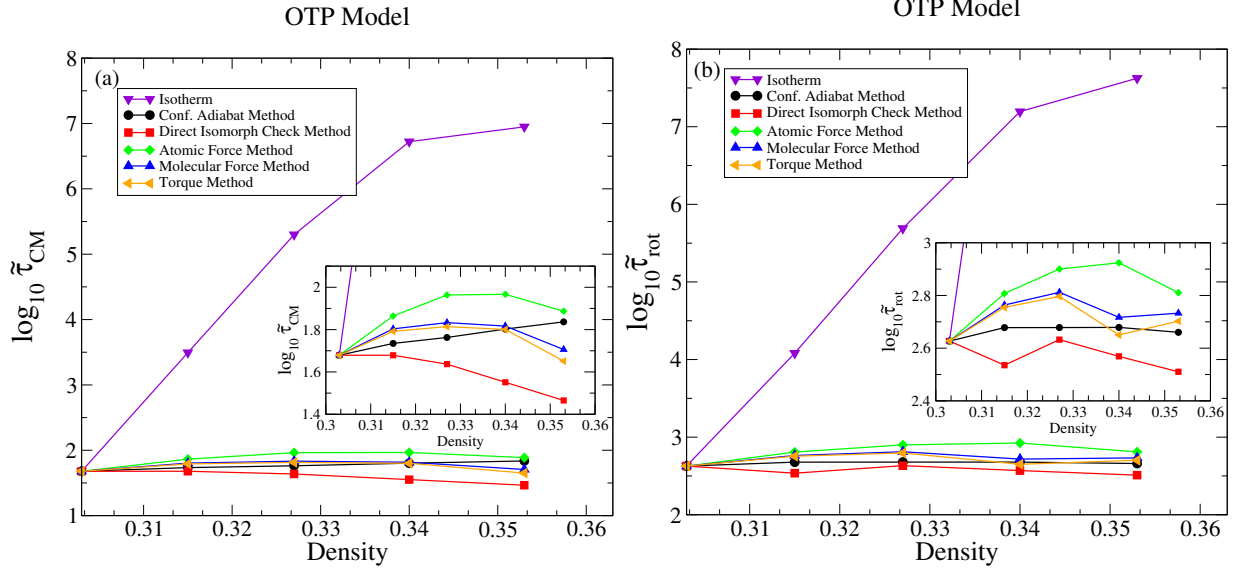


FIG. 9. Comparing the relaxation time as a function of the density in the OTP model along an isotherm and the various approximate isomorph methods. Both translational and rotational relaxation time are invariant compared to the isotherm (purple). (a) shows the translational relaxation time calculated by the intermediate scattering function. (b) shows a similar plot for the rotational relaxation time.

reference state point. The force methods involve in principle a single configuration and its uniformly scaled version, although we averaged over 152 configuration pairs in order to get better statistics and also to be able to estimate the uncertainty of the T_2 predictions. Such averaging is not going to be necessary if a much larger system is simulated than the presently studied (5000 molecules for ASD and IPL, and 3000 molecules for OTP). Apparently, both the intermolecular and intramolecular interactions play an important role in generating potentially isomorphic state points. In particular, the atomic forces are still affected by the intramolecular interactions, and we believe this is why the atomic-force method is not able to identify state points of approximately invariant reduced dynamics in some cases. On the other hand, the molecular-force method based on invariant reduced center-of-mass forces generally works well, while the torque method gave decent results in ASD model. For the IPL and OTP models, the torque method provides good results, as well.

Identifying isomorphs via three new methods is much simpler and computationally cheaper than the method in Ref [18]. The force methods for generating isomorphs have here only been tested on molecular systems composed of molecules with constraint bonds. The question whether the molecular-force based method works well for other molecular system,

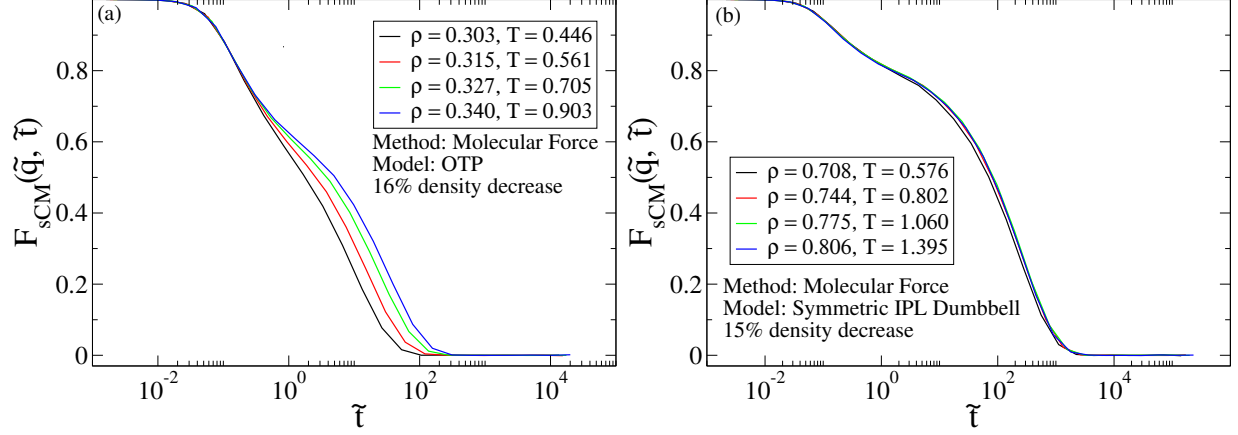


FIG. 10. Comparing the dynamics of two model (OTP, IPL) when the density decreased. (a) shows the incoherent intermediate scattering function illustrates that the dynamics of the OTP system is not invariant when state points are generated by decreasing the density. Here the reference state point is $(\rho_1, T_1) = (0.340, 0.903)$. Surprisingly, the molecular force method, which his best for the ASD and IPL methods and also for OTP when increasing the density, does not provide any isomorphic points. (b) shows testing the similar method on IPL model in similar process of decreasing the density. $(\rho_1, T_1) = (0.806, 1.395)$ is the starting point. The reduced dynamics quantity still has a perfect collapse and it is not effected by density changes.

e.g., with harmonic bonds, is important to investigate in future work.

-
- [1] Gnan,Nicoletta and Schröder,Thomas B. and Pedersen,Ulf R. and Bailey,Nicholas P. and Dyre,Jeppe C. "Pressure-energy correlations in liquids. IV. "Isomorphs" in liquid phase diagrams", The Journal of Chemical Physics, **131**, 234504 (2009).
 - [2] Dyre, Jeppe C., "Hidden Scale Invariance in Condensed Matter", The Journal of Physical Chemistry B, **118**, 10007-10024 (2014).
 - [3] Ingebrigtsen, Trond S. and Schröder, Thomas B. and Dyre, Jeppe C. "What Is a Simple Liquid?", Phys. Rev. X. **2**, 011011 (2012).
 - [4] Bailey,Nicholas P. and Bøhling,Lasse and Veldhorst,Arno A. and Schröder,Thomas B. and Dyre,Jeppe C. "Statistical mechanics of Roskilde liquids: Configurational adiabats, specific heat contours, and density dependence of the scaling exponent", The Journal of Chemical Physics. **139**, 184506 (2013).

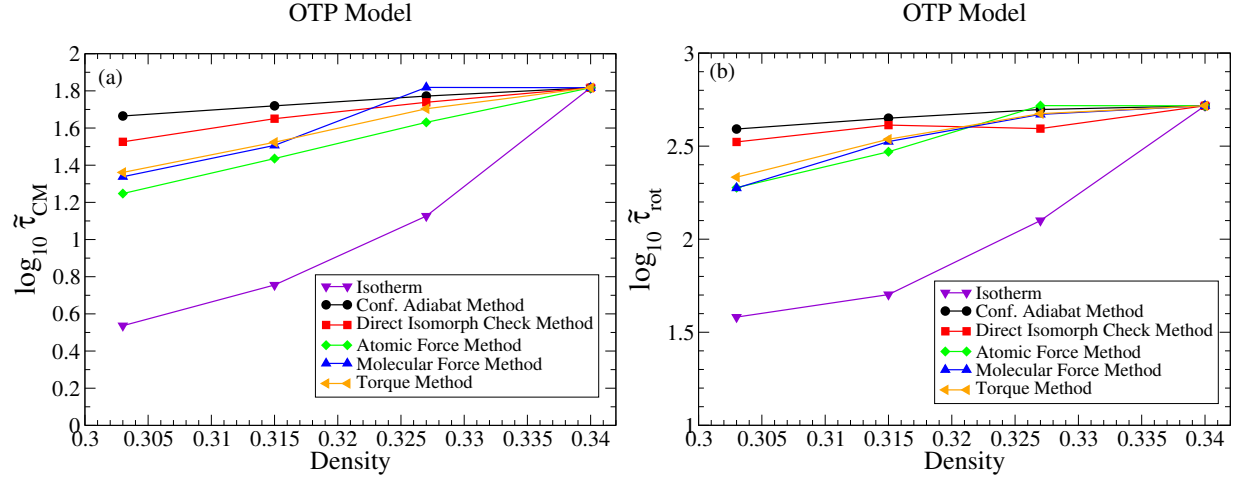


FIG. 11. Comparing the similar dynamical quantity represented in Fig. 9 given by five methods with isotherm. Again the variation of relaxation time is rather more invariant along isomorphs methods than isotherm (a) Shows the translational relaxation time as the function of density when we decrease the density and (b) shows the relevant quantities of rotational dynamics. In both panel the dynamics is more invariant along the configurational adiabats and direct isomorphs check methods in comparing with Fig. 9. Comparing the force methods shows they identify the proper isomorph state points only by increasing the density.

- [5] Flenner, Elijah and Staley, Hannah and Szamel, Grzegorz, "Universal Features of Dynamic Heterogeneity in Supercooled Liquids", *Phys. Rev. Lett.* **112**, 097801 (2014).
- [6] Prasad, Saurav and Chakravarty, Charusita, "Onset of simple liquid behaviour in modified water models", *The Journal of Chemical Physics*. **140**, 164501 (2014).
- [7] Bailey, Nicholas P. and Pedersen, Ulf R. and Gnan, Nicoletta and Schröder, Thomas B. and Dyre, Jeppe C. "Pressure-energy correlations in liquids. I. Results from computer simulations", *The Journal of Chemical Physics*, **129**, 184507 (2008).
- [8] Fragiadakis, D. and Roland, C. M. "On the density scaling of liquid dynamics", *The Journal of Chemical Physics*, **134**, 044504, (2011).
- [9] Koperwas, K. and Grzybowski, A. and Paluch, M. "The effect of molecular architecture on the physical properties of supercooled liquids studied by MD simulations: Density scaling and its relation to the equation of state", *The Journal of Chemical Physics*, **150**, 014501, (2019).
- [10] Fragiadakis, D. and Roland, C. M. "Intermolecular distance and density scaling of dynamics in molecular liquids", *The Journal of Chemical Physics*, **150**, 204501, (2019).
- [11] Schröder, Thomas B. and Dyre, Jeppe C. "Simplicity of condensed matter at its core: Generic

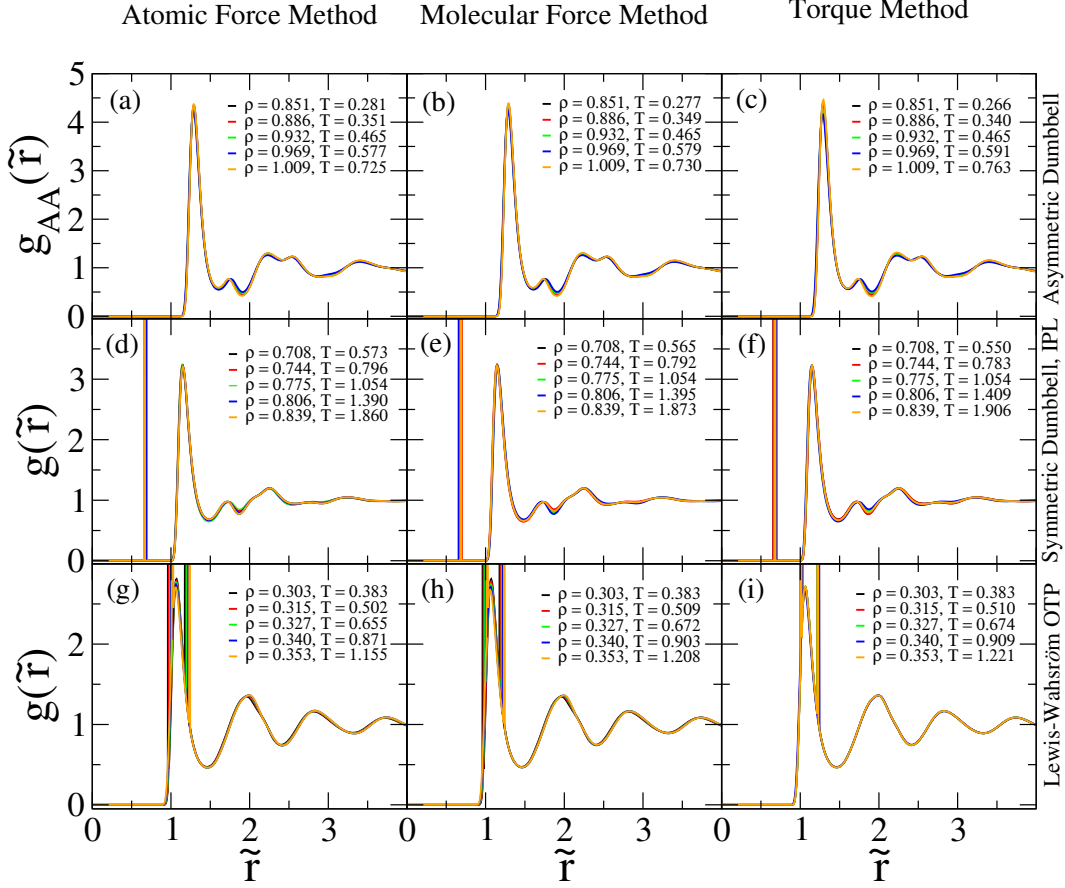


FIG. 12. Testing for invariance of the reduced-unit structure for the three different methods for the ASD, IPL, and OTP models. Results were averaged over 152 configurations to improve statistics. As previously, the configuration was scaled uniformly to the relevant density ρ_2 in order to determine the corresponding temperature T_2 . (a), (b), (c) show results for state points generated by the atomic and molecular force and torque method for ASD model. (d), (e), (f) show results for state points generated by the atomic and molecular force and torque for IPL model. (g), (h), (i) show results for state points generated by the atomic and molecular force and torque for OTP model.

- definition of a Roskilde-simple system”, The Journal of Chemical Physics, **141**, 204502 (2014).
- [12] Bailey, Nicholas P. and Pedersen, Ulf R. and Gnan, Nicoletta and Schröder, Thomas B. and Dyre, Jeppe C. ”Pressure-energy correlations in liquids. II. Analysis and consequences”, The Journal of Chemical Physics, **129**, 184508 (2008).
- [13] Schröder, Thomas B. and Bailey, Nicholas P. and Pedersen, Ulf R. and Gnan, Nicoletta and Dyre, Jeppe C. ”Pressure-energy correlations in liquids. III. Statistical mechanics and ther-

- modynamics of liquids with hidden scale invariance”, The Journal of Chemical Physics, **131**, 234503 (2009).
- [14] Pedersen, Ulf R. and Bailey, Nicholas P. and Schröder, Thomas B. and Dyre, Jeppe C. ”Strong Pressure-Energy Correlations in van der Waals Liquids”, Phys. Rev. Lett, **100**, 015701 (2008).
 - [15] Albrechtsen, Dan E. and Olsen, Andreas E. and Pedersen, Ulf R. and Schröder, Thomas B. and Dyre, Jeppe C. ”Isomorph invariance of the structure and dynamics of classical crystals”, Phys. Rev. B, **90**, 094106 (2014).
 - [16] Bacher, Andreas Kvist and Schröder, Thomas B. and Dyre, Jeppe C. ”The EXP pair-potential system. II. Fluid phase isomorphs”, The Journal of Chemical Physics, **149**, 114502 (2018).
 - [17] Costigliola, Lorenzo and Schröder, Thomas B. and Dyre, Jeppe C. ”Freezing and melting line invariants of the Lennard-Jones system”, Phys. Chem. Chem. Phys. **18**, 14678-14690 (2016).
 - [18] Ingebrigtsen, Trond S. and Schröder, Thomas B. and Dyre, Jeppe C. ”Isomorphs in Model Molecular Liquids”, The Journal of Physical Chemistry B, **116**, 1018-1034 (2012).
 - [19] Veldhorst, Arno A. and Dyre, Jeppe C. and Schröder, Thomas B. ”Scaling of the dynamics of flexible Lennard-Jones chains” The Journal of Chemical Physics, **141**, 054904 (2014).
 - [20] Wence Xiao and Jon Tofteskov and Troels V. Christensen and Jeppe C. Dyre and Kristine Niss. ”Isomorph theory prediction for the dielectric loss variation along an isochrone”, Journal of Non-Crystalline Solids, **407**, 190-195 (2015).
 - [21] Hansen, H.W. and Sanz, A. and Adrjanowicz, K. and Frick, B. and Niss, K. ”Evidence of a one-dimensional thermodynamic phase diagram for simple glass-formers”, Nature Communications, **9**, 518, (2018).
 - [22] Olsen, Andreas Elmerdahl and Dyre, Jeppe C. and Schröder, Thomas B. ”Communication: Pseudoisomorphs in liquids with intramolecular degrees of freedom”, The Journal of Chemical Physics, **145**, 241103, (2016).
 - [23] Schröder, Thomas B. ”Predicting Scaling Properties From a Single Fluid Configuration”, arXiv:2105.12258 [cond-mat.soft] (2021).
 - [24] Nicholas P. Bailey and Trond S. Ingebrigtsen and Jesper Schmidt Hansen and Arno A. Veldhorst and Lasse Böhling and Claire A. Lemarchand and Andreas E. Olsen and Andreas K. Bacher and Lorenzo Costigliola and Ulf R. Pedersen and Heine Larsen and Jeppe C. Dyre and Thomas B. Schröder. ”RUMD: A general purpose molecular dynamics package optimized to utilize GPU hardware down to a few thousands particles”, SciPost Physics, **3**, 038, (2017).

- [25] Jorge Nocedal; Wright Stephen J. "Numerical optimization", Springer, New York, NY, (2006).
- [26] William H. Press. "Numerical Recipes", Cambridge University Press, (2007).
- [27] Magnus R. Hestenes and Eduard Stiefel. "Methods of Conjugate Gradients for Solving Linear Systems", Journal of Research of the National Bureau of Standards, **49**, 2379, (1952).
- [28] Schrøder, Thomas B. and Pedersen, Ulf R. and Bailey, Nicholas P. and Toxvaerd, Søren and Dyre, Jeppe C. "Hidden scale invariance in molecular van der Waals liquids: A simulation study", Phys. Rev. E, **80**, 041502, (2009).
- [29] Dyre, Jeppe C. "Simple liquids' quasiuniversality and the hard-sphere paradigm", Journal of Physics: Condensed Matter, **28**, 323001, (2016).
- [30] Dyre, Jeppe C. "Perspective: Excess-entropy scaling", The Journal of Chemical Physics, **149**, 210901, (2018).